Journal of Solid State Chemistry **163,** 248–252 (2002)
doi:10.1006/jssc.2001.9399, available online at http://www.idealibrary.com on IDEAL®

First Principle Calculation of the Geometrical and Electronic Structure of Impurity-Doped β-$FeSi_2$ Semiconductors

Jun-ichi Tani[1] and Hiroyasu Kido

Department of Inorganic Chemistry, Osaka Municipal Technical Research Institute, 1-6-50 Morinomiya, Joto-ku, Osaka 536-8553, Japan

Received June 20, 2001; in revised form September 5, 2001; accepted September 14, 2001; published online November 27, 2001

The geometrical and electronic structures of impurity (Cr, Mn, Co, Ni)-doped β-$FeSi_2$ were investigated using first principles pseudopotential calculations based on generalized gradient approximation (GGA) density function theory. The calculated structural parameters depend strongly on the kinds of dopants and sites. The total energy calculations for substitution of dopants at the Fe_I and the Fe_{II} sites revealed that Mn prefers the Fe_I site, whereas Cr, Co, and Ni prefer the Fe_{II} site. The electronic structure is analyzed and discussed in terms of the atomic charges, bond overlap population, and total and partial densities of states (DOS). © 2002 Elsevier Science

Key Words: **$FeSi_2$; electronic structure calculations; doping; conduction type.**

INTRODUCTION

Transition metal silicides are of considerable interest from the viewpoint of their structural and functional applications. The semiconducting phase of iron disilicide (β-$FeSi_2$) has been studied as a material for thermoelectric conversion, because of its superior features such as its large Seebeck coefficient, low electrical resistivity, and chemical stability (1). There have been many attempts to dope additives into β-$FeSi_2$ to control its semiconducting properties. P-type conduction is found with doping with V, Cr, Mn, and Al doping and *n*-type with Co, Ni, Pt, and Pd doping (2–9).

Dusausoy *et al.* (10) determined an orthorhombic crystal system having 48 atoms per unit cell *Cmca* with the lattice constants $a = 0.9863$ nm, $b = 0.7791$ nm, and $c = 0.7833$ nm and the space group for β-$FeSi_2$. Figure 1 shows a unit cell of β-$FeSi_2$. There are two crystallographically inequivalent sites for Fe and Si (Fe_I, Fe_{II}, Si_I, Si_{II}). The unit cell contains 16 fomula units distributed over 8 Fe_I, 8 Fe_{II}, 16 Si_I, and 16 Si_{II}. The two types of Fe sites are coordinated by eight Si atoms with slightly different distances to Fe and have the point symmetries 2 (C_2) and *m* (C_s), respectively.

[1] To whom correspondence should be addressed. E-mail: tani@omtri.city.osaka.jp.

Kondo *et al.* measured the Mössbauer effect of ^{57}Fe in transition metal (Cr, Mn, Co, Ni)-doped β-$FeSi_2$ at room temperature, so as to examine the local atomic structure around Fe atoms (12). They found that Cr, Mn atoms nearly exclusively occupy the Fe_I site; and Co, Ni atoms tend to occupy the Fe_{II} site. Irmscher *et al.* have investigated bulk single crystals of β-$FeSi_2$ by electron paramagnetic resonance (EPR) spectoroscopy between 4 and 300 K (13). They concluded that Cr, Mn can occupy either of the two crystallographically inequivalent Fe sites; Co and Ni prefer one site. Szymanski *et al.* have investigated the preferential site occupation of Co in ion-implanted β-$FeSi_2$ layers at room temperature (14). A slight preference was found for one of the Fe sites, but it was not larger than 55:45. They concluded that their experimental results cannot support the conclusion of Kondo *et al.* that nearly all Co atoms enter selectively into Fe_{II} sites. The reason for the apparent discrepancies in the experimental work by these several researchers is not clear.

By studying mobility, we have recently shown that the small polaron model is valid for Co-doped, Ni-doped, and Cr-doped β-$FeSi_2$, whereas the ionized impurity scattering model is valid for Mn-doped β-$FeSi_2$. This result clearly suggests that the transport properties of impurity doped β-$FeSi_2$ depends sensitively on the kinds of dopant. However, to our knowledge, no theoretical data have been reported on the geometrical and electronic structure of impurity-doped β-$FeSi_2$, except a recent work on the electronic structure of partial or complete substitution of the Fe atoms in β-$FeSi_2$ with Ru, Os, or Cr (15).

In the present study, we performed quantum-mechanical first principle calculations of the Cr-, Mn-, Co-, and Ni-doped β-$FeSi_2$ within density functional theory to obtain precise information on the geometrical and electronic structures of this system. In the process of the calculation, the position of all atoms in the unit cell, as well as the lattice parameters, were allowed to relax by total energy minimization. At the optimized structure, the electronic structure was analyzed in terms of the atomic charges, bond overlap population, and total and partial densities of states.

0022-4596/02 $35.00

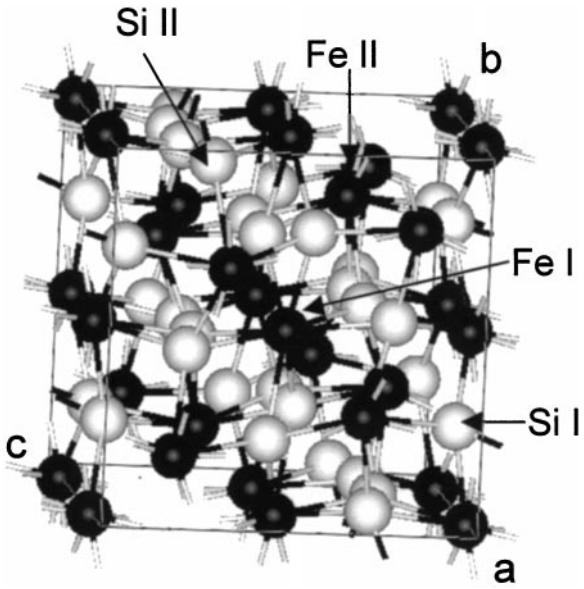

FIG. 1. Unit cell of β-$FeSi_2$. Black spheres represent Fe and white spheres represent Si. There are two crystallographically inequivalent sites of both Fe and Si (Fe_I, Fe_{II}, Si_I, Si_{II}).

DETAILS OF THE CALCULATIONS

Density functional theory (DFT) calculations within the pseudopotential and generalized gradient approximations (GGAs) were performed using the computer program CASTEP (Cambridge Serial Total Energy Package in Cerius2, Molecular Simulation, Inc.) (16). We constructed a primitive unit cell of 24 atoms (4 Fe_I, 4 Fe_{II}, 8 Si_I, 8 Si_{II}) with a face centering a–c plane (17). We replaced one of the eight sites of the Fe atoms by an impurity atom (M) in this primitive unit cell, that is, a composition of an impurity-doped β-$FeSi_2$ of $Fe_{0.875}M_{0.125}Si_2$. We expanded the valence electronic wave functions in a plane-wave basis set up to an energy cutoff of 560 eV, which converges the total energy of the unit cell to better than 1 meV/atom. In the total-energy calculations, integrations over the Brillouin zone were performed by using a $3 \times 3 \times 3$ Monkhurst–Pack set (18), which gives 14 symmetrized k points; again, the total energies converged to better than 1 meV/atom. The electron–ion interaction is described by a norm-conserving potential generated using the optimization scheme of Lin *et al.* (19).

RESULTS AND DISCUSSION

Table 1 shows the experimental and calculated structural parameters. The calculated values for nondoped β-$FeSi_2$ (relaxed structure) are in good agreement with the experimental results (unrelaxed structure) within $\pm 0.02\%$. The calculated structural parameters of impurity-doped β-$FeSi_2$ depend strongly on the kinds of dopants as well as the sites replaced by the dopants. Figures 2a to 2c show the calculated lattice constants a, b, c and the unit cell volume V against the atomic number of dopants. The unit cell volume V shows the minimum value at nondoped β-$FeSi_2$. The lattice constant a increased markedly by doping with Co, Ni, whereas the lattice constants b as well as c were almost constant. Hesse *et al.* reported a marked increase of lattice constant a in β-$Fe_{1-x}Co_xSi_2$ at the composition up to approximately $x = 0.12$, whereas lattice constants b as well as c are unaffected, and the lattice constants of β-$Fe_{0.88}Co_{0.12}Si_2$ were reported to be $a = 9.918$, $b = 7.798$, $c = 7.840$ (20). This experimental result is in fairly good agreement with our calculated results of β-$Fe_{0.875}Co_{0.125}Si_2$. The lattice constant a of $Fe_{0.875}Cr_{0.125}Si_2$ and $Fe_{0.875}Mn_{0.125}Si_2$ with Cr, Mn located at the Fe_I site was slightly larger than that located at the Fe_{II} site. However, the lattice constant a of $Fe_{0.875}Co_{0.125}Si_2$ and $Fe_{0.875}Ni_{0.125}Si_2$ with Co, Ni located at the Fe_I site was slightly smaller than that located at the Fe_{II} site. The unit cell volume V is independent of the site selection.

Table 2 shows the results of the total energy calculation of impurity-doped β-$FeSi_2$. A comparison of the computed total energies for substitution at the Fe_I and the Fe_{II} sites revealed that site I preferred $Fe_{0.875}Mn_{0.125}Si_2$, whereas site II preferred $Fe_{0.875}Cr_{0.125}Si_2$, $Fe_{0.875}Co_{0.125}Si_2$, and $Fe_{0.875}Ni_{0.125}Si_2$. Kondo *et al.* measured the Mössbauer effect of ^{57}Fe in transition metal (Cr, Mn, Co, Ni)-doped β-$FeSi_2$ at room temperature so as to examine the local atomic structure around Fe atoms. They found that Cr, Mn atoms nearly exclusively occupy the Fe_I site; and Co, Ni atoms tend to occupy the Fe_{II} site. The results of the total energy calculation for Mn-, Co-, and Ni-doped β-$FeSi_2$ seem to be in good agreement with the experimental results obtained by Kondo *et al.* However, in conflict with their results, our result for $Fe_{0.875}Cr_{0.125}Si_2$ is in good agreement

TABLE 1

The Calculated (Relaxed) and Experimental (Unrelaxed) (Ref. 10) structural Parameters for Nondoped and Impurity Doped β-$FeSi_2$

Samples	a (nm)	b (nm)	c (nm)	c/a	V (nm^3)
Nondoped (experimental)	0.9863	0.7791	0.7833	0.7942	0.6019
Nondoped (calculate)	0.9871	0.7777	0.7837	0.7939	0.6016
$Fe_{0.875}Cr_{0.125}Si_2$ (Fe_I site)	0.9870	0.7805	0.7875	0.7979	0.6067
$Fe_{0.875}Cr_{0.125}Si_2$ (Fe_{II} site)	0.9843	0.7818	0.7876	0.8002	0.6061
$Fe_{0.875}Mn_{0.125}Si_2$ (Fe_I site)	0.9884	0.7779	0.7842	0.7934	0.6030
$Fe_{0.875}Mn_{0.125}Si_2$ (Fe_{II} site)	0.9863	0.7793	0.7846	0.7955	0.6031
$Fe_{0.875}Co_{0.125}Si_2$ (Fe_I site)	0.9911	0.7789	0.7856	0.7927	0.6065
$Fe_{0.875}Co_{0.125}Si_2$ (Fe_{II} site)	0.9929	0.7777	0.7854	0.7910	0.6065
$Fe_{0.875}Ni_{0.125}Si_2$ (Fe_I site)	0.9975	0.7798	0.7874	0.7894	0.6125
$Fe_{0.875}Ni_{0.125}Si_2$ (Fe_{II} site)	0.9993	0.7790	0.7864	0.7870	0.6122

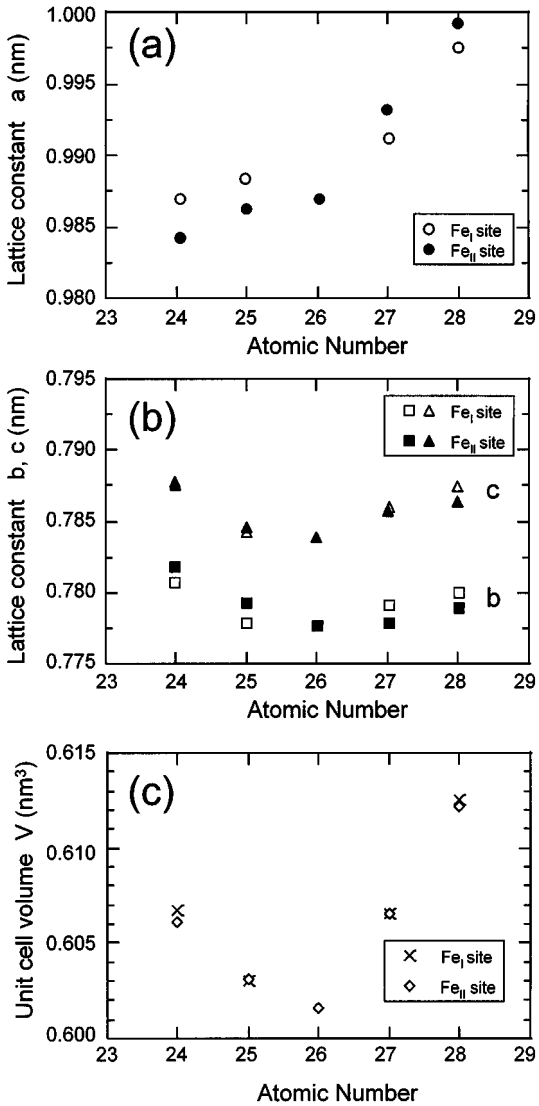

FIG. 2. Calculated lattice constants *a*, *b*, and *c* and the unit cell volume *V* against the atomic number of the dopants.

with the results of Ek *et al.* that the total energy for heavily doped Fe–Cr disilicides with Cr located at the more open Fe_{II} sites is lower than for substitution at Fe_I. Therefore,

TABLE 2
Total Energy Differences (ΔE) between $Fe_7M^{I}Si_{16}$ and $Fe_7M^{II}Si_{16}$ (M = Cr, Mn, Co, and Ni) and Stable Site of M

Samples	Stable Site	ΔE (meV)
$Fe_{0.875}Cr_{0.125}Si_2$	Fe_{II}	87.0
$Fe_{0.875}Mn_{0.125}Si_2$	Fe_I	10.6
$Fe_{0.875}Co_{0.125}Si_2$	Fe_{II}	40.0
$Fe_{0.875}Ni_{0.125}Si_2$	Fe_{II}	92.2

TABLE 3
Electronic Charges (in *e*) of the Atoms in Nondoped and Impurity Doped β-$FeSi_2$ Obtained by Mulliken Population Analysis

Samples	Fe_I	Fe_{II}	Si_I	Si_{II}	M_I	M_{II}
Nondoped unrelaxed	− 0.02	− 0.02	+ 0.02	0.00		
Nondoped (relaxed)	+ 0.01	0.00	+ 0.01	− 0.01		
$Fe_{0.875}Cr_{0.125}Si_2$ (Fe_I site)	− 0.02	− 0.03	+ 0.01	− 0.02	+ 0.24	
$Fe_{0.875}Cr_{0.125}Si_2$ (Fe_{II} site)	− 0.02	− 0.02	+ 0.01	− 0.01		+ 0.18
$Fe_{0.875}Mn_{0.125}Si_2$ (Fe_I site)	+ 0.01	− 0.01	0.00	− 0.02	+ 0.22	
$Fe_{0.875}Mn_{0.125}Si_2$ (Fe_{II} site)	0.00	0.00	0.00	− 0.02		+ 0.19
$Fe_{0.875}Co_{0.125}Si_2$ (Fe_I site)	+ 0.02	+ 0.02	+ 0.01	0.00	− 0.12	
$Fe_{0.875}Ni_{0.125}Si_2$ (Fe_{II} site)	+ 0.03	0.00	+ 0.01	− 0.01		− 0.13
$Fe_{0.875}Ni_{0.125}Si_2$ (Fe_I site)	+ 0.02	+ 0.04	+ 0.02	0.00	− 0.26	
$Fe_{0.875}Ni_{0.125}Si_2$ (Fe_{II} site)	+ 0.04	0.00	+ 0.01	0.00		− 0.27

Note. The value of charges is average of atoms at the same site in the primitive cell of 24 atoms.

theoretical calculations seem to predict that Cr occupy preferably at site Fe_{II} than Fe_I. The site preference of Cr is still an open question.

Table 3 shows the results of the Mulliken population analysis. The charge of unrelaxed nondoped β-$FeSi_2$ that both Fe_I and Fe_{II} indices a small negative value − 0.02, whereas Si_I indices a small positive value + 0.02. The charge of relaxed nondoped β-$FeSi_2$ that Fe_I and Si_I indices a small positive value + 0.01, Si_{II} a small negative value − 0.01. The atomic positions of nondoped β-$FeSi_2$ are relaxed until the forces on the atom are less than 0.001 eV/Å in the geometry optimization process. Therefore, this result suggests that the charge of Fe, Si depends not only on the sites (Fe_I, Fe_{II}, Si_I and Si_{II}), but also on the degree of the internal stress of individual atoms. The lattice and internal relaxation is found to have important effects on the results of the Mulliken population analysis. However, this calculation result clearly suggests that a large charge transfer from Fe to Si or from Si to Fe does not occur in nondoped β-$FeSi_2$.

However, in impurity-doped β-$FeSi_2$, Cr and Mn are positively charged in the range + 0.18 to + 0.24, whereas Co and Ni are negatively charged in the range − 0.12 to − 0.27. The charge of Fe_I, Fe_{II} depends on the dopants and the sites. The charge of Fe_{II} indicates a small negative value in the range of − 0.03 and 0.00 for $Fe_{0.875}Cr_{0.125}Si_2$ and $Fe_{0.875}Mn_{0.125}Si_2$, respectively. In contrast, the charge of Fe_{II} indicates a small positive value in the range of 0.00 and + 0.04 for $Fe_{0.875}Co_{0.125}Si_2$ and $Fe_{0.875}Ni_{0.125}Si_2$,

TABLE 4

The Distances and Bond Overlap Population between Impurity (M) and Si Atoms, Which is the Average Value between M and Si Atoms Located at MSi_8 Octahedra Unit

	Fe_I site		Fe_{II} site	
M	r (M_I–Si) (nm)	Bond overlap population	r (M_{II}–Si) (nm)	Bond overlap population
Fe	0.2359	0.165	0.2381	0.150
Cr	0.2403 (+ 1.9%)	0.005	0.2428 (+ 2.0%)	− 0.005
Mn	0.2356 (− 1.5%)	0.123	0.2384 (+ 0.1%)	0.113
Co	0.2373 (+ 0.6%)	0.190	0.2399 (+ 0.7%)	0.178
Ni	0.2384 (+ 1.1%)	0.220	0.2412 (+ 1.3%)	0.205

Note. Deviations from the Fe–Si distance are shown in parentheses.

respectively. This result clearly suggests that, by impurity doping, charge transfer (e^-) from Cr, Mn to Fe_I, Fe_{II} as well as from Fe_I, Fe_{II} to Co, Ni occurs. The polarity of Fe_I, Fe_{II} strongly depends on the kinds of dopant. On the other hand, the charges of Si_I, Si_{II} indicate 0.00– + 0.02, − 0.02– + 0.00, respectively. The polarity of Si_I, Si_{II} seems to not be much influenced by the kinds of dopants and the sites.

The characteristic of the electronic interaction can be studied by the bond overlap population analysis. The distortion of the lattice around the impurity was analyzed in terms of the MSi_8 octahedra unit. Table 4 shows the average value of the bond distance and bond overlap population between M and Si atoms, which is the average value between M and Si atoms located at the MSi_8 octahedra unit. The positive and negative values of the population indicate bonding and antibonding characteristics of the interactions between two atomic orbitals. The mean distance of M-Si is slightly changed by substituting an impurity into Fe_I and Fe_{II}. The average value of the bond overlap population of Fe_I–Si indicates 0.165, which is slightly larger than that of Fe_{II}–Si, 0.150. The difference between the absolute values of the bond overlap population at Fe_I–Si and Fe_{II}–Si may be simply due to the difference between the lengths of the Fe_I–Si and Fe_{II}–Si bonds. The average length of the Fe_I–Si bond is 0.2359 nm, which is slightly shorter than that of the Fe_{II}–Si bond, 0.2381 nm. The bonds of Cr–Si and Mn–Si are weaker than the Fe–Si bond, whereas the bonds of Co–Si and Ni–Si are stronger than the Fe–Si bond. The average overlap population between Cr and Si atoms is much closer to zero, showing very weak interaction between Cr and Si.

The Si–Si bonds are in the range of 0.245 and 0.259 nm, which is longer than Fe–Si. However, the average of the bond overlap population of Si–Si shows 0.30, which is larger than the value of Fe–Si. The bond overlap population of Si–Si is not much influenced by the kinds of dopant. This result suggests that Si–Si bonds would be strong in the β-$FeSi_2$ structure, rather than Fe–Si bonds.

Differences in the DOS curves for the nonrelaxed and relaxed structures were slight and not important. The total DOS plot for the relaxed structure is shown in Fig. 3a. Energy is measured relative to the Fermi level $E_F = 0$ eV (dot line). The primitive cell of nondoped β-$FeSi_2$ exhibited the indirect band gap of 0.79 eV between the Y point in the valence band and the point located at the $2/5(Z\Gamma)$ line in the conduction band that agrees with the calculations of Miglio *et al.* and Clark *et al.* (21, 22). This value of band gap is in fairly good agreement with the experimental one of 0.83–0.89 eV (23).

Figures 3b to 3i show the total DOS plots for impurity-doped β-$FeSi_2$. In comparing the eight figures and Fig. 3a,

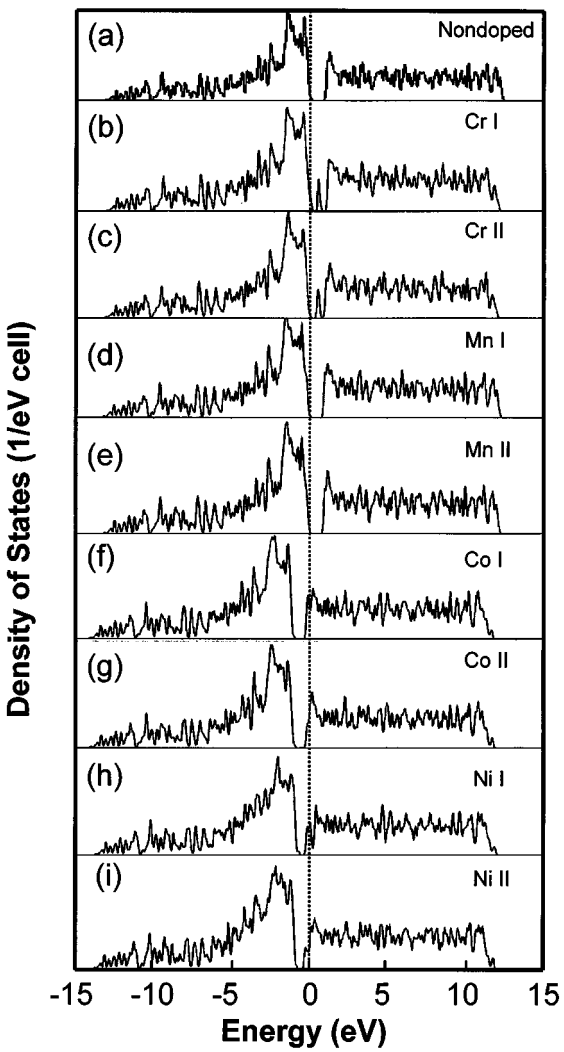

FIG. 3. Total density of states (DOS) of β-$Fe_{0.875}M_{0.125}Si_2$: (a) nondoped, (b) M = Cr (at Fe_I site), (c) M = Cr (at Fe_{II} site), (d) M = Mn (at Fe_I site), (e) M = Mn (at Fe_{II} site), (f) M = Co (at Fe_I site), (g) M = Co (at Fe_{II} site), (h) M = Ni (at Fe_I site), and (i) M = Ni (at Fe_{II} site).

we found that the electronic structures of the impurity doped β-$FeSi_2$ crystals have the same band shape as that of nondoped β-$FeSi_2$, that is, there is little change in electronic structures except in the energy regions near or between the band edge.

We verified from the analyses of the site-decomposed DOS as well as the partially decomposed DOS that these impurity levels originate mainly 3*d* orbitals from impurity atoms, and their states are found to be largely delocalized. For Cr, Mn-doped β-$FeSi_2$, E_F exists at the top of the valence band. For Cr-doped β-$FeSi_2$, we can clearly see a sharp impurity level produced between the valence band and the conduction band. For Mn-doped β-$FeSi_2$, a sharp impurity level is produced at the top of the valence band, and the impurity level is not fully occupied by electrons. This fact suggests that a small hole pocket exists in the valence band. Therefore, the calculations predict of carrier type that the conduction type of Cr, Mn-doped β-$FeSi_2$ shows *p*-type. On the other hand, for Co, Ni-doped β-$FeSi_2$, E_F exists at impurity levels near the bottom of the conduction band. Therefore, the calculation predicts that the conduction type of these materials shows *n*-type. These calculations of carrier type are in good agreement with our previously reported experimental results on the Hall effect (7–9).

4. CONCLUSION

The geometrical and electronic structures of impurity (Cr, Mn, Co, Ni)-doped β-$FeSi_2$ were investigated using first principles pseudupotential calculations based on generalized gradient approximation (GGA) density function theory. The calculated structural parameters depend strongly on the kinds of dopants and sites. The total energy calculations for substitution of dopants at the Fe_I and the Fe_{II} sites revealed that that Mn prefers the Fe_I site, whereas Cr, Co, and Ni prefer the Fe_{II} site. Cr and Mn are positively charged in the range $+0.18$ and $+0.24$, whereas Co, Ni are negatively charged in the range -0.12 and -0.27. This result clearly suggests that, by impurity doping, charge transfer (e^-) from Cr, Mn to Fe_I, Fe_{II} as well as from Fe_I, Fe_{II} to Co, Ni occurs. We found that the electronic structures of the doped β-$FeSi_2$ crystals have the same band shape as that of nondoped β-$FeSi_2$; that is, there is little change in electronic structures except in the energy regions near or between the band edge. The predictions of carrier type from the DOS are in good agreement with our previously reported experimental results on the Hall effect.

ACKNOWLEDGMENT

The authors thank Dr. K. Chiba (Ryoka Systems Inc.) for his technical support.

REFERENCES

1. D. M. Rowe, "CRC Handbook of Thermoelectrics," p. 287. CRC Press, New York, 1995
2. R. M. Ware and D. J. McNeill, *Proc. IEE* **111,** 178 (1964).
3. U. Birkholz and J. Schelm, *Phys. Status Solidi* **27,** 413 (1968).
4. I. Nishida, *Phys. Rev. B* **7,** 2710 (1973).
5. T. Kojima, *Phys. Status Solidi A* **111,** 233 (1989).
6. M. Komabayashi, K. Hijikata, and S. Ido, *Jpn. J. Appl. Phys.* **30,** 331 (1991).
7. J. Tani and H. Kido, *J. Appl. Phys.* **84,** 1408 (1998).
8. J. Tani and H. Kido, *J. Appl. Phys.* **86,** 464 (1999).
9. J. Tani and H. Kido, *Jpn. J. Appl. Phys.* **38,** 2717 (1999).
10. Y. Dusansoy, J. Protas, R. Wandij, and B. Roques, *Acta Crystallogr. B* **27,** 1209 (1971).
11. S. Kondo, M. Hasaka, T. Morimura, and Y. Miyajima, *Nucl. Instrum. Methods Phys. Res. B* **76,** 383 (1993).
12. S. Kondo, M. Hasaka, T. Morimura, and Y. Miyajima, *Physica B* **198,** 322 (1994).
13. K. Irmscher, W. Gehlhoff, Y. Tomm, H. Lange, and V. Alex, *Phys. Rev. B* **55,** 4417 (1997).
14. K. Szymanski, L. Dobrzynski, A. Andrejczuk, R. Chrenowicz, A. Vantomme, S. Degroote, and G. Langouche, *J. Phys. Condens. Matter* **8,** 5317 (1996).
15. J. van Ek, P. E. A. Turchi, and P. A. Sterne, *Phys. Rev. B* **54,** 7897 (1996).
16. CASTEP Users Guide. Molecular Simulations Inc., San Diego, CA, 1998.
17. A. B. Filonov, D. B. Migas, V. L. Shaposhnikov, N. N. Dorozhkin, G. V. Petrov, V. E. Borisenko, W. Henrion, and H. Lange, *J. Appl. Phys.* **79,** 7708 (1996).
18. H. J. Monkhorst and J. D. Pack, *Phys. Rev. B* **13,** 5188 (1976).
19. J. S. Lin, A. Qteish, M. C. Payne, and V. Heine, *Phys. Rev. B* **47,** 4174 (1993).
20. J. Hesse and R. Bucksch, *J. Mater. Sci.* **5,** 272 (1970).
21. L. Miglio and V. Meregalli, *J. Vac. Sci. Technol. B* **16,** 1604 (1998).
22. S. J. Clark, H. M. Al-Allak, S. Brand, and R. A. Abram, *Phys. Rev. B* **58,** 10389 (1998).
23. H. Lange, *Phys. Status Solidi B* **201,** 3 (1997), and reference therein.